Evidence for time and directional enhancements of multimuon cosmic-ray events

J. Bartelt,* H. Courant, K. Heller, T. Joyce,
M. L. Marshak, E. A. Peterson, K. Ruddick, and M. Shupe
School of Physics, University of Minnesota, Minneapolis, Minnesota 55455

D. S. Ayres, J. Dawson, T. Fields, E. N. May, L. E. Price, and K. Sivaprasad†
High Energy Physics Division, Argonne National Laboratory, Argonne, Illinois 60439
(Received 29 October 1984)

We have observed 1.05×10^6 single-muon and 6869 multimuon events deep underground with the Soudan 1 nucleon-decay detector. The single-muon flux is consistent with isotropy and with results of previous experiments. We have found indications of bursts of multimuon events, particularly from a direction near Cygnus X-3. These bursts arrive from an extended angular region of $30° \times 30°$. The size of the angular region and the lack of a corresponding effect in the single-muon events are difficult to understand. In addition, there is weaker evidence for an excess in the time-integrated multimuon flux near the north galactic pole. We have evaluated the possibility that these effects are caused by random or systematic errors.

I. INTRODUCTION

Particle-detector arrays have often been used to search for flux-enhanced directions of high-energy cosmic-ray air-showers. Data from such arrays have also been used to search for time-dependent effects which could be attributed to nonsteady sources of cosmic-rays, either periodic or episodic.[1] Until recently, reports of point-source-like anisotropies or temporal nonuniformities in high energy cosmic-rays have not been confirmed by independent experiments.

This situation has changed during the past several years. Both Samorski and Stamm[2] and Lloyd-Evans et al.[3] have reported experimental evidence for a localized, pulsed source of high-energy ($>10^{15}$ eV) radiation. Based on the apparent repetition period of 4.8 hours and the direction (with a reconstruction accuracy of 1° in Ref. 2) of this radiation, its source has been identified as the x-ray binary Cygnus X-3. Consequently, the observed signals (as detected in air-showers with energies of order $10^{15}-10^{16}$ eV) have been attributed to high-energy photons. This hypothesis is based upon: (a) previous observations of similarly pulsed low energy gamma rays from Cygnus X-3; (b) a distribution of electrons suggesting an initial interaction point very high in the atmosphere for those extensive air-showers which show the effect; and (c) the randomizing effect of the galactic magnetic fields, which suggests that any traceable primaries from as far as Cygnus X-3 must be uncharged. (In particular, from the radio data[4], the distance to Cygnus X-3 is estimated to be greater than 10 kpc, which is of order 10^3 times the galactic magnetic gyroradius for a 10^{16} eV charged particle.)

Recently, Protheroe et al. have published[5] similar evidence for periodic pulses of high-energy photons from Vela X-1, located in the southern-hemisphere sky. Two reports[6,7] of single-episode bursts of high-energy cosmic-ray air-showers also imply nonrandom sources, but whether these sources have properties similar to Cygnus X-3 and Vela X-1 is not clear. Neither confirmatory nor contrary evidence for either of these bursts has appeared in the literature.

In this paper, we report on the results of a search for source-like directional and time modulation in a large sample of cosmic-ray data collected with the Soudan 1 proton-decay detector during the period September 1981 through November 1983. This underground detector, located at a depth of 590 m or 1800 m water equivalent, is sensitive to single-muon events with a cosmic-ray primary (proton) median energy of $\approx 5 \times 10^{12}$ eV and multiple, parallel muon events (called in this paper "multimuon events") with a median energy of $\approx 10^{14}$ eV. Its effective angular resolution for multimuon events is 0.8°.

In searching for source-like effects in our data, we have concentrated on the multimuon events, which are more likely to originate from high-energy primaries. Heavy nuclear primaries are also more efficient at inducing multimuon events than are protons.

As will be described below, our data appear to contain some statistically significant evidence for an episodic enhancement of the multimuon-producing cosmic-ray component. Calculation of the significance of the observed effect is complicated because our analysis originated with no a priori hypotheses. As a result, the parameters of the effect are derived from the data themselves. Nonetheless, a particular directional region of angular width of $\approx 30° \times 30°$, centered at right-ascension $\alpha = 295°$, declination $\delta = 60°$ has shown evidence during our observation period for several bursts of multimuon events. These bursts appear only very improbably to be statistical fluctuations of a uni-

form background.

The direction of this effect is approximately 20° away from Cygnus X-3. It is also near the galactic plane and lies at approximately a right angle to the direction of the galactic center. Thus this direction is close in orientation to the axis of the local spiral arm, to the velocity vector describing the galactic motion of our solar system and to the direction of the local galactic magnetic field. This angular region is also quite near the overhead direction (local sidereal time of 261° at 50° N latitude) at the time of the burst observation described in Ref. 6. Another possible coincidence is that we detected an apparent peak of episodic multimuon activity from this region about six days before a major radio outburst[8] from Cygnus X-3. Our single-muon data, however, do not show any enhancement similar to that in our multimuon events.

There are also other suggestions of anisotropies in our data. In particular, the region adjacent to the galactic north pole seems to contribute a time-integrated excess of multimuon events, particularly events with very high multiplicity. In considering the results which follow, one should remember that photons are not expected to be a source for multimuon events. Most primary photons produce electromagnetic showers,which have only a small hadronic component. Since underground muons result primarily from pion decay, the events which we observe are conventionally ascribed to proton or heavy nuclear primaries, both of which are presumably charged.

It is, however, possible that multimuon events could be initiated by very-high-energy neutrons. Because of neutron decay, the neutron energy spectrum will be flatter than the proton energy spectrum. The decay length for a 10^{15} eV neutron is about 10 pc. We know of no data regarding the flux of high-energy neutrons in the cosmic-rays incident on the earth.

In the following sections, we describe our detector and our data-analysis procedures in considerable detail. This description should permit the reader to form an independent judgment of the statistical and systematic significance of the effects which we have observed and of the likelihood that they may be related to some of the other phenomena reported in the references.

II. DETECTOR

The Soudan 1 proton-decay detector is located at 48° N latitude, 92° W longitude at a depth of 590 m, which is equivalent to 1800±40 m of water. It is shown schematically in Fig. 1 and is also described in Ref. 9. The detector consists of 3456 horizontal steel proportional tubes, each 2.8 cm in diameter, spaced by approximately 4 cm in each direction throughout a block of 31 metric tons of heavy concrete. The overall dimensions of the array are 2.9 m by 2.9 m by 1.9 m high. The tubes are arranged in 48 layers, with alternate layers turned by 90° in order to provide two views of each event.

Events were recorded upon a trigger composed of time-coincident hits in any proportional tube in any three out of four adjacent layers. Time of day and date were recorded
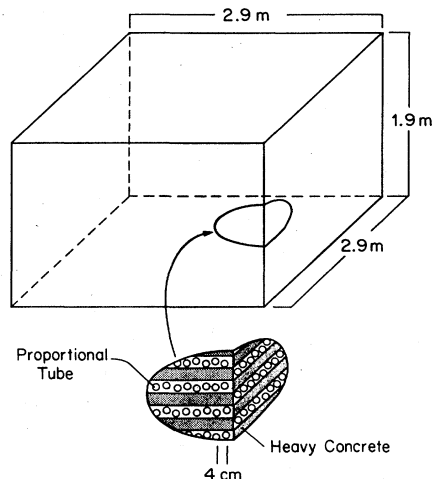

FIG. 1. A schematic view of the Soudan 1 detector.

with the proportional-tube data for each event. The live-time was determined by a 10 kHz, crystal-controlled oscillator. During detector operation, the livetime ratio varied from 85 to 93 percent as the overall trigger rate changed with atmospheric pressure, proportional-tube gas quality, and electronic instabilities. The dead time resulted from the proportional-tube readout and recording process.

The two-track resolution as determined from the data is 4 cm. The detector angular resolution depends on track length and orientation. From the measured angular deviations between presumably parallel tracks (shown in Fig. 2), we have deduced that the angular resolution of our detector (standard deviation) is ≈0.8°. The measured space-angle difference between two parallel muon tracks is $\sqrt{2}$ larger or ≈1.2°. For comparison, we estimate that muons produced with 700 GeV each will experience the following contributions to their measured rms space-angle difference before they enter the detector: (a) hadronic production and decay processes, 0.04°; (b) differential bending between μ^+ and μ^- in the earth's magnetic field, 0.01° to 0.04° depending on orientation relative to the earth's magnetic field and the height of the interaction; and (c) multiple Coulomb scattering in the rock overburden, 0.32°. Consequently, the angular resolution in the sky is dominated by the detector properties. We estimate from Fig. 2 that the rms space-angle resolution of the primary direction as measured by the average direction of a muon pair is ≈0.8°.

Fig. 3 shows examples of single- and multiple-muon events as recorded in our detector. The array of points represents the lattice of proportional tubes. The view with odd layer numbers is from the north looking south; the view with even layer numbers is from the west looking east. Those tubes with valid hits in Fig. 3(a) are indicated by numbers and letters (1-9, A-Z; A=10, B=11, etc.) which show the number of time periods (approximately 180 ns each) that the tube output was above threshold (giving a measure of the ionization deposited). Other symbols indicate invalid tube outputs. The dots (.) on every eighth tube are merely a visual aid for tube location. The
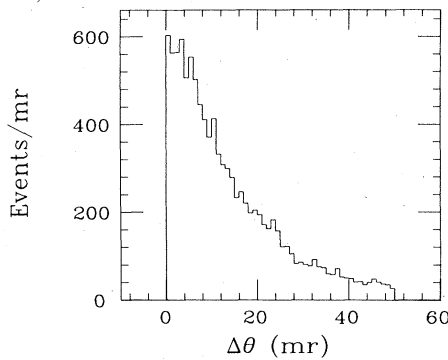
FIG. 2. The distribution of the projected angular difference in milliradians between tracks in multimuon events. Only events with two tracks in each view are used for this plot, and data from both views are plotted.

Previous underground muon experiments most similar to Soudan 1 in terms of spatial and angular resolution are the Park City detector[12], the Kolar-gold-field detector[13] and the Mayflower Mine experiment[14]. The Park City detector covered about 10 times the area of Soudan 1, but had poorer spatial resolution (30 cm as opposed to 4 cm). That experiment was only sensitive to trajectories at zenith angles >50°. The Kolar detector also had coarser spatial resolution (10 cm) than Soudan 1 and collected most of its data at deeper locations. The Mayflower Mine experiment is shallower (507 m water equivalent) than Soudan 1 and has only reported data on single-muon fluxes.

III. DATA HANDLING

The data sample reported here represents a live time of 0.92 years. After computer reconstruction and classification by physicists, the sample includes 1.05×10^6 single-muon and 6869 parallel multimuon events. The overall data-handling procedures are described in Ref. 9.

The vast majority of muon events show single, non-interacting tracks. Multimuon candidates were first selected by a computer algorithm which picked those events with more than 8 proportional-tube hits that did not reconstruct to a single, linear track. Reconstruction was then attempted on about 20000 such candidates using a multimuon hypothesis. All of these events, successfully reconstructed or not, were scanned by physicists to check on the selection of multimuon events and to correct, if

tube hits in Fig. 3b are represented by a number or letter indicating to which track the hit has been assigned by the analysis procedure.

Ninety-five percent of the primaries producing multimuon events at the Soudan 1 depth have energies $>10^{13}$ eV. The maximum primary energy expected at the one-event level in our data sample is 5×10^{16} eV, based on the standard flux-energy relation measured in other experiments.[10] As mentioned above, we have estimated from a Monte Carlo calculation of the atmospheric cascade and propagation of muons through the earth[11] that the median proton primary energies for our data are 5×10^{12} eV and 10^{14} eV for single- and multimuon events, respectively.

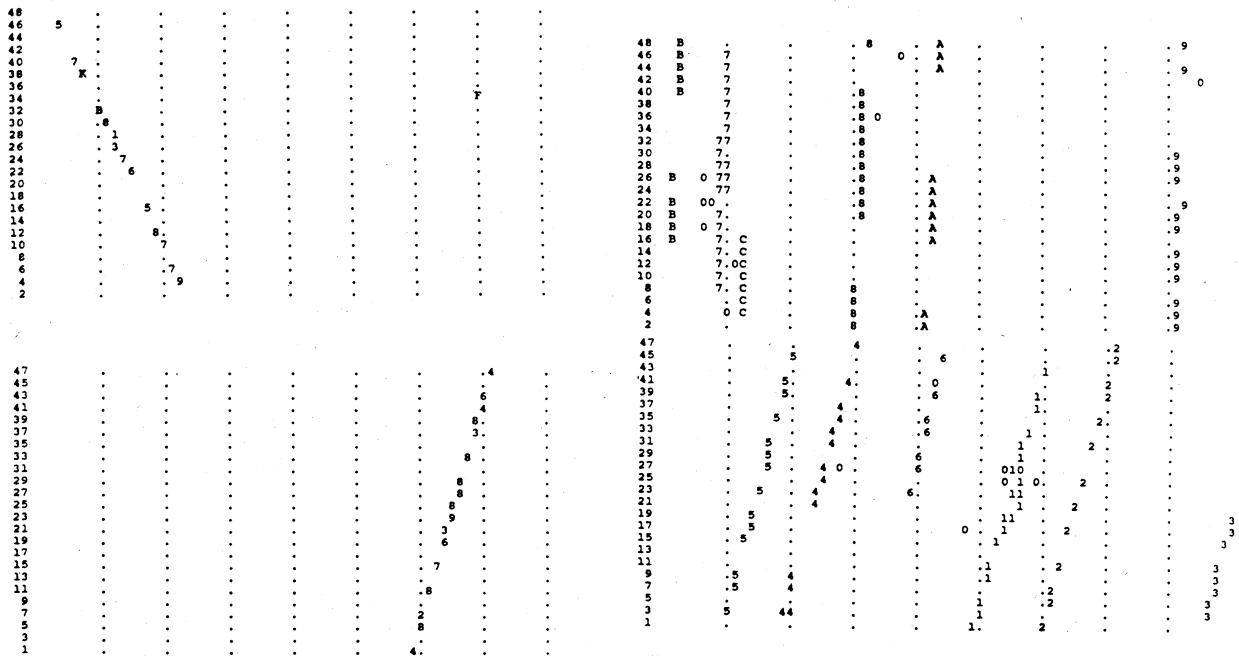
FIG. 3. The two views of the proportional tubes hit in a single (a) and a multimuon (b) event. The numbers and letters for the single-muon event indicate the time duration that the signal from each tube was above threshold. The numbers and letters for the multimuon event indicate the track assignment of each proportional tube. Odd-numbered layers are viewed from the north; even-numbered layers are viewed from the west.

necessary, the reconstruction of the selected events. The selection process used the following two criteria: (a) A track was defined as a minimum of three proportional-tube hits (track length >16 cm) forming a straight line and not starting or stopping within the detector. (b) A multimuon event required at least two such tracks, in at least one view, which did not cross each other in either view within 5 m of the detector face.

After selection and correction, the direction of arrival in local coordinates of each event was calculated from the two orthogonal views. This information and the time of arrival were used to calculate the right-ascension and declination for each event. Because the Soudan 1 detector has proportional tubes only at right angles, the individual tracks of a multimuon event cannot always be directly correlated in the two views. This limitation does not affect the determination of the source direction for parallel tracks.

IV. SINGLE-MUON INTENSITY DISTRIBUTION

Although the primary emphasis of this report is the multiple, parallel muon events, with their higher primary energy spectrum, the Soudan 1 detector also recorded 1.05 x 10^6 single-muon events. Single muons have been observed for many years deep underground without any confirmed reports of substantial anomalies. However, the good statistics and high directional accuracy of the Soudan 1 data make a summary report on the single-muon flux useful. Perhaps more importantly, the single-muon events provide a contemporaneous basis for comparison with the multiple-muon events. The thrust of this section, then, is that the single-muon flux recorded by the Soudan 1 detector is well understood, in good agreement with previous results and thus provides a useful baseline for comparison with the multimuon events.

Fig. 4 shows the local-zenith-angle distribution for the single-muon events. Only tracks crossing a central spherical region (radius 1.25 m) of the detector have been used in this plot (293 000 events total) in order to eliminate acceptance biases due to detector corners and edges. The azimuthal distribution, which is not shown, is in agreement with the principal features of the local geology. The detector is situated below a ridge approximately 40 m high, whose longitudinal axis is close to the east-west direction. The ridge is associated with a 150-200 m wide, near-vertical fault region containing iron-bearing rocks and very localized, dense hematite ore bodies. North and south of this fault region, the rock is relatively homogenous and consists primarily of Ely greenstone, a metamorphosed volcanic rock. The correlations between the measured single-muon intensities and the surface terrain have permitted a determination of the orientation of the detector to an accuracy of better than 1°, in agreement with the results of a conventional survey. By comparing these intensities with other data,[15,16] the average rock density has been found to be 2.93±.05, with the density north of
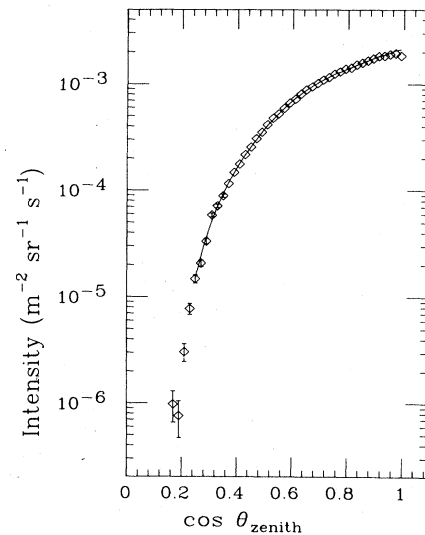

FIG. 4. The zenith-angle distribution for single-muon events. The line represents an empirical fit to the data. The intensity $I(\theta)=A \sec \theta \ E^{-\gamma}$ where $E=e^{bR} - 1$. R is the slant depth at angle θ. E is proportional to the minimum energy required to reach depth R, corresponding to an ionization loss $-dE/dx = c + fE_\mu$. E_μ is distributed according to the integral energy spectrum of the muons in the atmosphere. The fit parameters are $b = 823\pm2$ m^{-1}, $\gamma = 2.58\pm0.01$, $A = 2.43\pm0.12$ x 10^{-3} m^{-2} sr^{-1} s^{-1}.

the fault region about 5 percent greater than that of the southern rock. From these fits, and from chemical analysis of the local rocks, we determined that $<Z^2/A>$ for the overburden is 6.0 ± 0.1. By comparison, "standard rock" has a density of 2.65 and a $<Z^2/A> = 5.5$.

The right-ascension dependence of the single-muon intensity is plotted in Fig. 5. The approximately 5 percent variation is due principally to detector off-time. The detector was turned off at various intervals over two years for various reasons. The on-off effect was not completely averaged out over the course of these observations. This single-muon right-ascension distribution provides an acceptance calibration for the study of right-ascension variations in the multimuon flux, which is reported in later
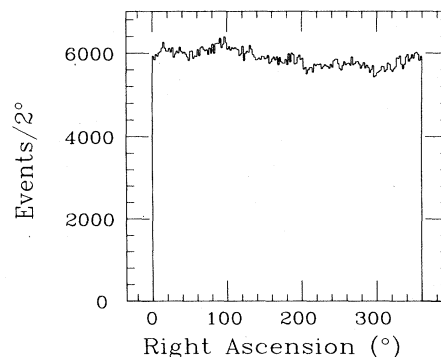

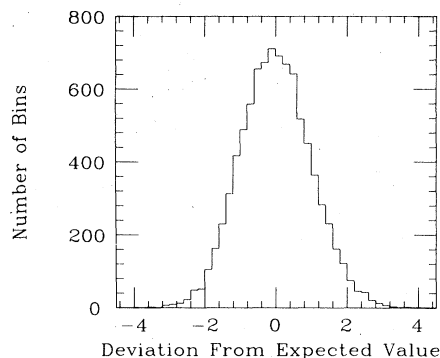FIG. 5. The right-ascension distribution for single-muon events over the entire data run.

FIG. 6. The distribution of deviations from expected value for numbers of single-muon events in $2° \times 2°$ bins. The independent variable is plotted in units of the square root of the number of events expected in each bin.
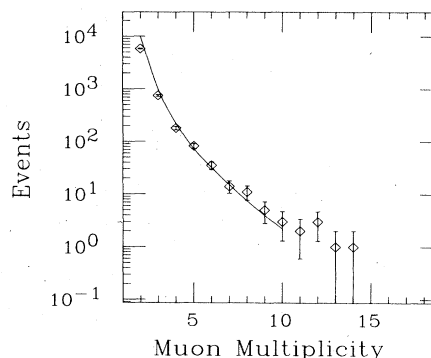

FIG. 7. The muon multiplicity distribution for multimuon events. The curve represents the results of a Monte Carlo calculation described in the text.

sections.

Fig. 6 shows the results of a search for time-integrated sources in the single-muon flux. The method used was as follows: The data were divided into $2° \times 2°$ bins in the right-ascension α and the declination δ. This bin size was chosen because it is somewhat larger than the overall angular resolution of the experiment. The expected number of counts $E(\alpha, \delta)$ was computed using the equation

$$E(\alpha, \delta) = N_\delta(\alpha) \times N_\alpha(\delta) / N_{tot} \qquad (1)$$

where $N_\delta(\alpha)$ is the number of events summed over δ for a given $2°$ bin in α, $N_\alpha(\delta)$ is the number of events summed over α for a given $2°$ bin in δ and N_{tot} is the total number of events. The 8820 bins with more than 20 expected counts are included in the plot in Fig. 6. The independent variable D is the deviation between the observed value and the expected value in a bin measured in units of the square root of the expected value. The χ^2 calculated from the data in Fig. 6 is 8716.0 for 8819 degrees of freedom, which corresponds to a probability of 80 percent, indicating that the measured flux is well described by Eq. 1.

Fig. 6 is therefore consistent with the hypothesis of a purely isotropic flux. For a single source to be observed in this data sample, at for example the 4σ level, an additional flux equal to at least 35 percent of the steady background for the region $30° < \delta < 60°$ would be required. This flux corresponds to a threshold level for a point source of ≈ 40 detected events per year, which represents a flux of $\approx 6 \times 10^{-11}$ cm^{-2} s^{-1}. In this regard, we note that the gamma-ray flux from Cygnus X-3 estimated[2] for $E > 2 \times 10^{13}$ eV is an order of magnitude smaller than this flux. This low flux, combined with the expected low efficiency for photons to produce muons, should mean that photon-induced events from Cygnus X-3 are unobservable as underground muon events in the single-muon data.

V. MULTIMUON INTENSITY DISTRIBUTION

The muon multiplicity distribution for multimuon events is shown in Fig. 7. This distribution reflects properties of the primary composition, the atmospheric cascade, the detector size and the detector depth. It is not possible to determine uniquely any parameters of physics interest from a single distribution of this type. However, the observations can be compared with a Monte Carlo model which incorporates parameters known from other observations. The curve in Fig. 7 was calculated using the previously mentioned Monte Carlo program,[11] using the depth, density, and chemical-composition parameters derived from the single-muon data. The input parameters included a primary flux of only protons with the known primary energy spectrum (dN/dE proportional to $E^{-2.71}$ up to 3×10^{15} eV and $E^{-3.0}$ at higher energies). The good agreement between the Monte Carlo model and the data indicate that the observed multimuon events are mostly consistent with the expectations from conventional cosmic-ray sources.

A search for time-integrated point sources of multimuon events can be made by using the same procedure as described for the single-muon events in the previous section. We have divided the multimuon events into $2° \times 2°$ bins in α and δ. The expected number of events in each bin has been calculated according to Eq. 1, using multimuon fluxes instead of single-muon fluxes.

The results of this search are negative. There are 6396 $2° \times 2°$ bins containing more than 0.5 expected events. The number of events found in these bins is consistent with Poisson fluctuations from a uniform distribution. In particular, 32 bins are expected by chance to contain sufficient events that the bin has a Poisson probability <0.005, 13 bins are expected to have a probability <0.002, and 6 bins are expected to have a probability <0.001. The observed numbers of bins are 18, 8, and 1, respectively. Similarly, there are 2870 bins containing more than 1.0 expected events. The observed (and expected) numbers of bins with Poisson probabilities <0.005, <0.002, and <0.001 are 12 (14), 5 (5), and 1 (3), respectively.

The test described above is sensitive only if multimuon events are induced by primaries such as photons which have no angular dispersion. If multimuon events are dispersed in direction, as would be the case if they

resulted from charged primaries, this test should also be performed using larger bins. The α, δ coordinate system is simple to use because in it the effect of the earth's rotation is straightforward. However, the galactic coordinate system (galactic latitude b^{II} and galactic longitude l^{II}) presumably has a simpler physical meaning for cosmic-ray primaries and should also be considered. For these reasons, we have searched for time-integrated multimuon flux enhancements using a range of angular bin size and both the α, δ and the b^{II}, l^{II} coordinate systems.

Since the experimental acceptance is not uniform in either galactic coordinate, this analysis requires a more complex evaluation of the number of events that might be expected from each direction given both a random, isotropic flux and the actual detector acceptance both in space and time. These "background" rates were determined by constructing 100 background data ensembles, each equivalent in normalization to the actual observed data, in the following manner: The single-muon events were used as a contemporaneous measure of the observation time for multimuon events. For each background ensemble, 0.6428 percent (the multimuon-event-to-single-muon-event ratio) of the single-muon events were chosen by generating a random number for each event. The times of day and dates of these events were used as the times of fake multimuon events. The remaining parameters of each fake event were determined by randomly selecting one real multimuon event and combining its local direction (altitude and azimuth) with the previously chosen time. This process was then repeated 100 times with different random-number seeds, in order to generate the 100 ensembles.

The "background" (i.e. the number of counts to be expected in the absence of directional or time enhancements) for any given binning or cutting of the real data sample was then determined by applying the same binning and cutting procedure to the sum of the 100 background ensembles and dividing the contents of each bin by 100. The variance for each bin of the background was determined by calculating the mean-square deviation of the contents of that bin using the 100 background ensembles. This method of determining the random background was also used for the time-dependent studies described in the next section.

The results of these broad bin searches for time-integrated source enhancements can be summarized as follows: There is no particular binning in α and δ which shows any statistically unexpected results. For example, in a 30° × 30° binning, there is a bin which is 3.6 standard deviations (σ) above the expected value, but such a deviation is not unexpected considering the number of bins examined. When the events are binned using the coordinates b^{II} and l^{II}, small enhancements are observed which merit interest more because of their special position than because of their statistical significance.

Fig. 8a shows the number of multimuon events as a function of $\sin b^{II}$. The sine function is used to minimize solid angle variation. The larger enhancement appears at

the north galactic pole ($\sin b^{II} = 1$). 352 events are observed instead of an expected 300 ± 17.2 events for $\sin b^{II} > 0.95$, a 3 standard deviation effect. (There are 153 events over a background of 119 ± 10.8 events for $\sin b^{II} > 0.98$). We note that although the north galactic pole is a special direction with respect to the galaxy, it is not a special point in local detector coordinates nor is it near any edges of the acceptance. There is a weak indication of a second, broader enhancement (640 events over a background of 597) near the galactic plane ($0 < \sin b^{II} < 0.15$), but this indication is not statistically significant (1.7 standard deviations).

The enhancement near the north galactic pole is more apparent when the highest muon multiplicity events are selected. The source direction distribution for events with 5 or more muons is shown in Figs. 8b and 9. From a Monte Carlo model, we estimate that the mean primary energy associated with these events is $\approx 2 \times 10^{15}$ eV. Fig. 9 shows a two-dimensional, equal-area projection. The expected number of events is roughly uniform for bins which are side-by-side, that is, which have equal values of δ. Nonetheless, the single bin $180° < \alpha < 200°$, $20° < \delta < 40°$, which includes the north galactic pole, contains 11 events instead of an expected 2.9 events (2.5 events if this bin is not included in calculating the expected value). The Poisson probability for this observation is 2.2×10^{-4},
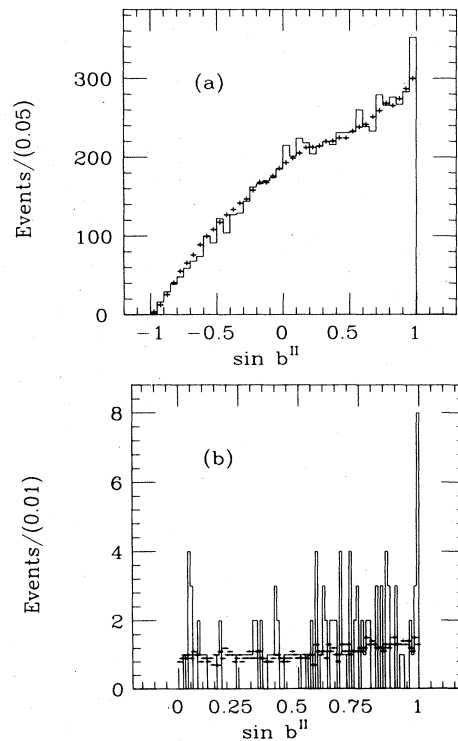

FIG. 8. (a) The distribution of multiple-muon events as a function of $\sin b^{II}$, where b^{II} is the galactic latitude (b) the same distribution for events with 5 or more muons. The solid line represents data; the crosses represent the background calculated as described in the text.
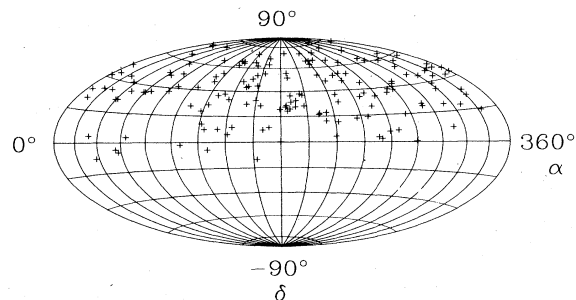
FIG. 9. A Hammer-Aitoff equal-area projection of the right-ascension (horizontal axis running from 0° to 360°) and the declination (vertical axis running from -90° to 90°) for multimuon events with 5 or more muons.

which then needs to be multiplied by the number of bins considered (≈ 100) to estimate an overall probability of 2.2 percent.

In summary, the time-integrated multimuon data are in general agreement with expectations under the assumption of a random, uniformly distributed flux. The only apparent anomalies, which may be purely statistical fluctuations, are seen in a histogram with galactic latitude as the independent variable. The most striking effect here is at the north galactic pole. This excess seems to be more pronounced for the highest-multiplicity events.

VI. SEARCH FOR TIME-DEPENDENT EFFECTS

Optical- and radio-astronomy data contain many examples of both periodic and episodic phenomena. As mentioned earlier, periodic and episodic events have also been observed in cosmic-ray air-shower data. Because of these known effects, we have searched the Soudan 1 multimuon data sample for time-dependent effects. The procedure we have used is essentially an autocorrelation analysis, in which we count the number of multimuon events from a given direction within a given time interval.

The choice of the size for direction and time bins for such an analysis is, of course, arbitrary. A number of sizes of angular bin were used, but because no narrow effects were seen, we have finally chosen rather broad angular bins, 30° on a side. For the time bin, we have used 12000 s for most of our analysis. This length is close to the longest possible time interval for which the detector can maintain good acceptance on a fixed point in the sky. On average, about 2.5 multimuon events from all directions would be expected in such a period.

We have made systematic checks to determine that the results reported are not peculiar to the exact values of these bin sizes. We have found that our conclusions remain the same even if the angular or time bin widths are changed. The time width is particularly insensitive and even a factor of two or three shorter time does not result in significantly different conclusions.

Multiple multimuon events or "bursts" were then defined by the following procedure: Starting a clock with a multimuon event, the subsequent 12000 s were scanned for those multimuon events coming from the same α, δ bin (30° x 30°). *Each event was counted only once,* either as a starting event or as a subsequent member of a burst of events (multiple multimuon event) within 12000 s. On average, the number of multimuon events expected within 12000 s after an initial event in the same 30° x 30° angular bin is about 0.13.

The background mean and variance have been estimated by using the same 100 background ensembles described in the previous section. The standard deviation of the background count is not just the square root of the mean but approximately $\sqrt{2}$ times that amount (as expected) because multiple multimuon events are generally two-fold.

The data have been analyzed in five groups, chosen according to the declination of the events. These groups are roughly symmetric about the peak acceptance in declination, which is equal to the detector latitude of +48°. The groups are (1) $\delta < -15°$, (2) $-15° < \delta < 15°$, (3) $15° < \delta < 45°$, (4) $45° < \delta < 75°$, and (5) $\delta > 75°$. Table 1 gives the distribution of the events among the five groups and among the burst multiplicities over the entire run period from September 1981 through November 1983. The events in each group were separately analyzed for time-dependent effects.

The most interesting results were observed for the two most highly populated groups, namely 3 and 4. Tables 2 and 3 and Figs. 10 and 11 display the number of multimuon events which are contained in "bursts" of 2 or more events in the same angular bin within 12000 s. Only in Fig. 11 do we see any significant excess of the number of burst events over background. This plot shows that one bin (280° < α < 310°) has 86 burst multimuon events compared to an expected number (i.e., for random time dependence) of 49.6±10.0 events, a 3.6σ excess.

Fig. 12 shows a histogram of multimuon events contained in bursts as a function of time over the entire run for $45° < \delta < 75°$, 280° < α < 310°. A large fraction (41/86) of the events occurred during the period of May

Table I: Time distribution of multimuon events for entire data sample.

Declination bin	Total multimuon events	Number of multimuon events in each burst multiplicity			
		1	2	3	4
<-15°	16	16	0	0	0
-15° - 15°	1014	844	152	18	0
15° - 45°	2887	1985	744	138	20
45° - 75°	2608	1976	538	90	4
>75°	344	338	6	0	0

Table II. Multimuon events in bursts as a function of right ascension (30° bins) for declinations between 15° and 45° for entire data run.

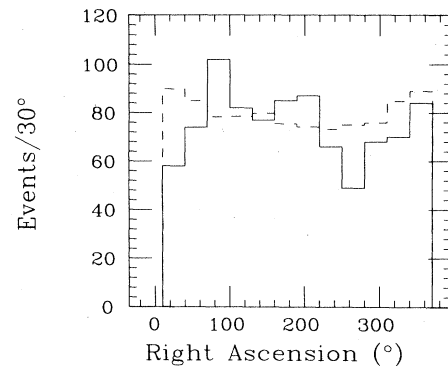| Right ascension (deg)	Observed events	Background	Background rms deviation
25	58	89.8	12.9
55	74	84.9	12.5
85	102	78.3	11.5
115	82	78.5	11.5
145	77	79.8	13.6
175	85	75.5	11.1
205	87	74.2	12.4
235	66	73.2	12.0
265	49	75.0	12.0
295	68	75.9	12.3
325	70	84.8	13.1
355	84	88.9	12.0

FIG. 10. The right-ascension distribution for each multimuon event which occurred in a burst for the declination band $15° < \delta < 45°$ for the entire data run. The dashed line represents the expected background calculated as described in the text.

through September 1982. This time span was approximately 1/4 of the duration of the entire data-collection period.

Therefore, we have reanalyzed the data using only this quarter of the run, making an identical date cut on both the real data and the 100 background ensembles. The results are shown in Table 4 and Fig. 13. The peak in the right-ascension distribution is now more pronounced, containing 41 multimuon events in bursts versus a background expectation of 13.7 ± 5.2. The particular numbers of observed multimuon events, backgrounds and Poisson probabilities are:

two-event bursts   14 obs.,   6.15 bkgd.
$P(\geq 14, 6.2) = 4.5 \times 10^{-3}$

three-event bursts   3 obs.,   0.45 bkgd.
$P(\geq 3, 0.45) = 1.1 \times 10^{-2}$

four-event bursts   1 obs.,   0.01 bkgd.
$P(\geq 1, 0.01) = 1.0 \times 10^{-2}$

The product of these probabilities is thus 5×10^{-7}. This value is, however, an underestimate of the joint probability because of permutations among the numbers of doubles, triples and quadruples. An overestimate of the proba-

bility can be obtained by calculating the Poisson probability of observing greater than or equal to 18 bursts with an expected number of 6.61. This probability is 1.8×10^{-4}. A maximum-likelihood analysis, described later, yields a probability of 3×10^{-5}, which lies between the bounds estimated here. This probability must then be multiplied by the number of right-ascension bins (12) times the number of declination bins (5) times the number of run-time bins (4), giving an overall probability of 0.7 percent. The total multimuon flux in this same bin during this same period is 89 events with a background of 61.2 ± 7.8 events, a 3.6σ enhancement. This signal is also visible with reduced significance as a time-integrated excess for the entire data run, similar to the effect described earlier at the north galactic pole. That latter phenomenon is not enhanced by a time-dependent analysis of the type described here.

Fig. 14 indicates that the excess events in the second quarter of the data run may have really occurred in two relatively short periods, one in May/June and the other in September 1982. This plot shows the daily distribution of the events in the peak bin for the months April through October 1982, along with the number of live seconds each
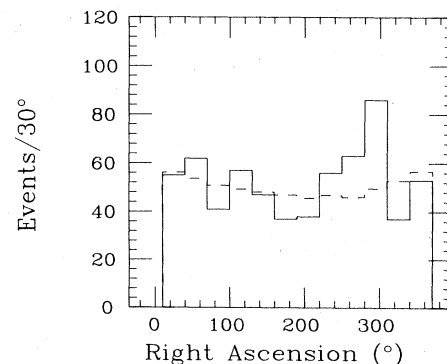
Table III. Multimuon events in bursts as a function of right ascension (30° bins) for declinations between 45° and 75° for entire data run.

Right ascension (deg)	Observed events	Background	Background rms deviation
25	55	56.2	10.2
55	62	53.7	9.6
85	41	50.8	10.5
115	57	49.3	10.7
145	47	48.1	9.6
175	37	46.9	11.2
205	38	45.6	10.6
235	56	46.8	9.8
265	63	46.0	9.2
295	86	49.6	10.0
325	37	52.7	10.1
355	53	56.7	9.7

FIG. 11. The right-ascension distribution for each multimuon event which occurred in a burst for the declination band $45° < \delta < 75°$ for the entire data run. The dashed line is the expected background.
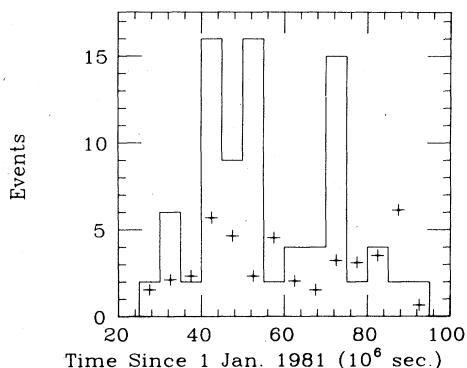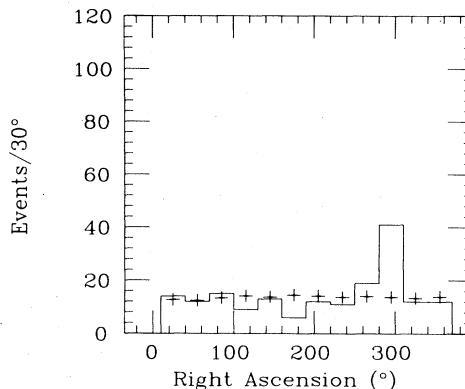
FIG. 12. The time-of-arrival distribution (in units of 10^6 s since 1 January 1981 UT) for multimuon events in bursts for $45° < \delta < 75°$, $280° < \alpha < 310°$. The crosses show the expected background rate.

FIG. 13. The right-ascension distribution for each multimuon event which occurred in a burst for the declination band $45° < \delta < 75°$ for the second quarter of the data run. The crosses represent the expected background calculated as described in the text.

month. Note that in May and September, a total of 13 bursts containing 30 multimuon events from this same bin were observed in a total exposure of 2.88×10^6 live seconds. In the intervening months, June, July, and August, with a live time of 3.75×10^6 s, only 5 bursts occurred, containing 11 events. By contrast, in April and October, the detector operated for 3.50×10^6 live seconds with no multimuon bursts observed in this bin. The expected number of bursts in this angular bin in 2.9×10^6 live seconds is 2 ± 1 containing 4 multimuon events.

Some further details about the burst multimuon events are provided in Fig. 15. This figure includes those bursts which occurred during the periods May 1 through June 10 and September 1 through September 30. In Fig. 15(a), the cosine of the separation angle between successive events in a burst is plotted and compared with a similar quantity calculated for the background events. The time separation for successive events in a burst is shown in Fig. 15(b), again with a distribution for the background. The data appear to cluster near $\cos \theta = 1$ somewhat more than background. The time clustering for the data is quite clear with 16 of 19 intervals (84 ± 9 percent) less than 6000 s, while only 54 ± 2 percent of the background intervals fall

within the first 6000 s. These internal characteristics of bursts further support the hypothesis that these events are different from the majority of multimuon events.

In order to extract additional information concerning the time duration of the multiple-multimuon-event signal as well as to further evaluate its statistical significance, we have made a likelihood analysis of the multiplicity distribution (number of multimuon events in each burst) for the 86 observed multimuon events. The signal (above a steady background) was parametrized by its time-integrated multimuon event intensity and by its duty cycle. The latter quantity was defined as the fraction of the (April-September 1982) period during which an additional, localized source was radiating at an assumed constant rate. A Poisson function was used for the distribution of event multiplicity in bursts. A Poisson function is not completely correct, because of the daily modulation of the detector acceptance for any specific source direction due to the rotation of the earth. However, a separate Monte Carlo calculation indicated that a Poisson distribution is a good approximation to the actual experimental situation.

Table IV. Multimuon events in bursts as a function of right ascension (30° bins) for declinations between 45° and 75° for second quarter of data run.

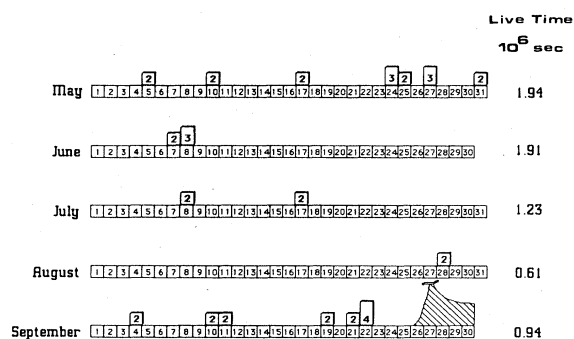| Right ascension (deg)	Observed events	Background	Background rms deviation
25	14	12.7	5.0
55	12	12.4	5.0
85	15	13.3	4.8
115	7	14.1	5.7
145	11	13.7	4.9
175	6	14.5	5.4
205	12	14.1	4.9
235	11	13.7	5.1
265	19	14.0	5.2
295	41	13.7	4.8
325	12	13.3	5.4
355	12	13.9	5.0

FIG. 14. The daily distribution of multimuon events in bursts for the months of May, June, July, August, and September 1982 UT. No bursts were observed in April or October 1982. The shaded area represents the radio outburst described in the text.
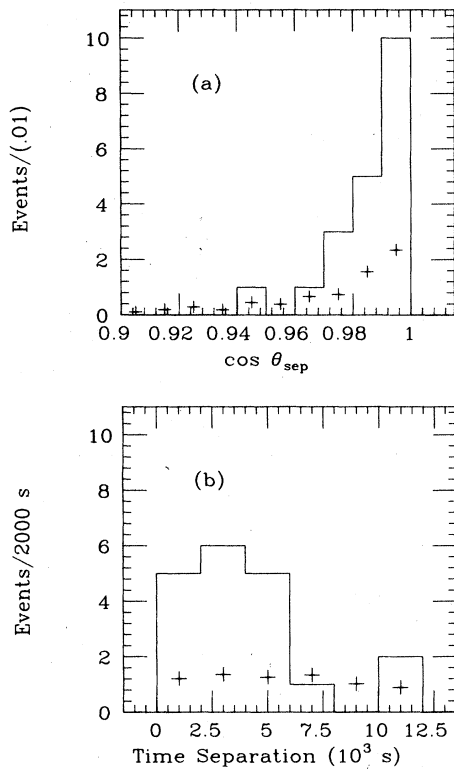
FIG. 15. Some details on the multimuon events in bursts. (a) shows the cosine of the separation angle between successive events within a burst. (b) shows the time separation calculated for the same pairs of events. The crosses show an estimate of the background.

Fig. 16 shows the likelihood contours which were obtained in this model, using the fixed background estimates described above. The probability that the signal in this angular bin represents a statistical fluctuation can be estimated as 3×10^{-5}, using the fact that $-2\ln L$ (where L is the likelihood function) is expected to follow a χ^2
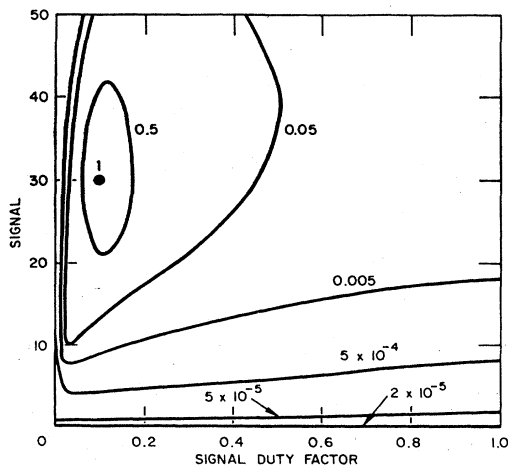
distribution. This probability lies well within the bounds discussed earlier. When multiplied by the number of bins (240 as described earlier), this analysis yields an overall probability of 0.7 percent that the effect is a statistical fluctuation. The most likely signal strength is 30 ± 8 multimuon events and the most likely duty factor is $0.10^{+0.06}_{-0.04}$ i.e. from 5 to 20 days total signal duration. This analysis may be oversimplified if the correlation period of a burst is considerably less than $12\,000$ s.

A process which produces multimuon bursts should also contribute to the single-muon event rate, since, for any given primary-cosmic-ray energy, the probability of observing a single-muon event is more than that of observing a multimuon event. Of course, the background in the single-muon data may be so large that establishing the existence of such a burst signal there is impossible. In order to minimize such background effects, we have analyzed the single-muon data during the four $12\,000$ s periods during which the three triple and one quadruple multimuon sequences occurred in May, June, and September 1982. The background was estimated by using the declination distribution for all single-muon events and normalizing to the same total area. The results of this analysis are shown in Fig. 17, which reveals no significant excess in the bins (but rather a deficit!) for $45° < \delta < 75°$. From Fig. 17, we can derive an upper limit for the ratio single-muon/multimuon events of <0.5 at 95 percent confidence. Monte Carlo simulations using the cosmic-ray model previously described indicate that the single-to-multimuon ratio in the Soudan 1 detector for proton primaries is 350, 28, and 6 for primary energies of 10^{13}, 10^{14}, and 10^{15} eV, respectively. The ratio for heavier primaries will be considerably lower.

This rather stringent limit on an enhancement in the single-muon events therefore seems to support one of three hypotheses: (a) the primary energy associated with multimuon events in the bursts is $>10^{15}$ eV, (b) the parent particles are heavy nuclei with high energy, or (c) the
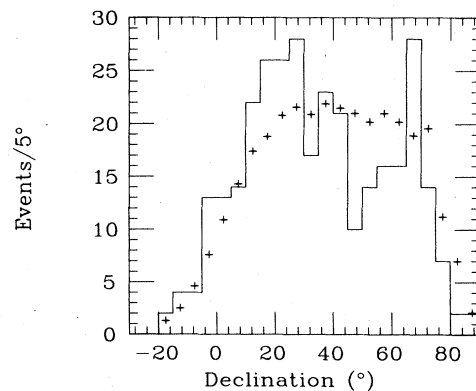

FIG. 16. The likelihood-function contours described in the text. Each contour is labelled by its relative likelihood.

FIG. 17. The declination distribution for single-muon events during the $12\,000$ s periods of the three 3-multimuon-event bursts and the one 4-multimuon-event burst. The crosses show the declination distribution for all single-muon events normalized to equal area.

multimuon bursts or single-muon data observed are biased by statistical or systematic fluctuations. In fact, hypotheses (a) and (b) are not supported by the observation that multimuon events contained and not contained in bursts have apparently identical muon multiplicity distributions.

We note that a major radio outburst of Cygnus X-3 occurred on September 27 ± 1, 1982, approximately 6 days after the strongest grouping of multiple multimuon events (2 doubles and 1 quadruple multiple multimuon events on 3 consecutive days) in our data. The radio outburst lasted about 10 days and was comprised of several successive peaks. The time profile of this radio signal is shown in Fig. 14. The Cygnus X-3 phases[17] of these events are (in order) 0.53, 0.71, 0.34, 0.63, 0.23, 0.44, 0.54, and 0.59.

The question of whether collimated bursts occur from directions other than the one cited above is addressed by Fig. 18. Here we plot the cosine of the separation angle between pairs of multimuon events which occurred within 5000 s of each other. (This shorter time period is used to improve the signal-to-background ratio.) Any pair in which either event occurred in the angular bin described previously has been eliminated from this plot. The evidence in the plot is inconclusive. There are of 180 pairs in the bin $\cos\theta > 0.98$ over a background of 164 ± 13, which is less than a two-standard-deviation effect. The question of whether bursts come from other directions needs further investigation.

VII. SYSTEMATIC UNCERTAINTIES

We have performed numerous checks with negative results to find systematic difficulties with the observations reported here. The signature of a multimuon event is distinctive and we believe that the possibility that such an event can be simulated by noise is remote. We have visually inspected each individual event within a burst to be sure that each event is unique and that no event is a mere repetition of an earlier one slightly modified by some computer or program error. We have also carried out two
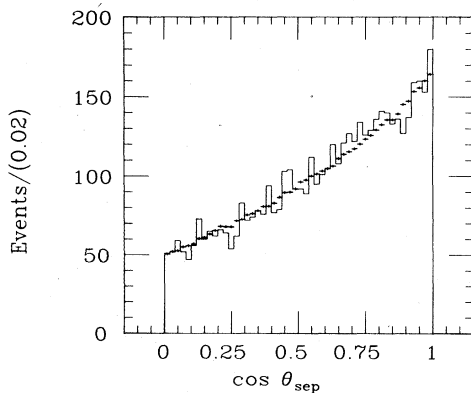

FIG. 18. The distribution of multimuon events as a function of the cosine of the separation angle for all pairs of events within 5000 s, except for events within the bin $45° < \delta < 75°$, $280° < \alpha < 310°$. The crosses indicate the calculated background distribution.

semi-independent analyses of the data using different computer programs at two different institutions.

To determine the arrival direction of events in celestial coordinates, we have used standard techniques to determine the position of the detector on the surface of the earth and the orientation of the detector relative to standard geodetic coordinates. By far the larger uncertainty is in the second measurement. Although it is easy to establish the vertical direction underground, propagating an azimuthal reference angle down a mineshaft is more difficult. We estimate an uncertainty of $\pm1°$ in the azimuthal orientation of the detector. However, this uncertainty does not affect the significance of the reported results.

The reconstructed direction in celestial coordinates is, of course, directly dependent on knowledge of the time of arrival. This time was kept by an independent quartz-crystal-controlled clock, which was interrogated by the data-acquisition computer. This clock provided both time and date information. It was set by standard radio-broadcast time information and was certainly accurate to better than one minute over the entire experiment. The resultant angular uncertainty is about 0.25°, much less than the orientation uncertainty described above. A second check on the clock was that each event was assigned a run number and event number in sequence by the data-acquisition computer. We have found no discrepancies between monotonically increasing run/event number and monotonically increasing time.

We also note that over the two-year duration of the experiment (or even the six months of the most significant effect), a particular direction in the sky is not associated with any particular direction in the detector. No extraordinarily active region in the detector or even a hole in the rock from the surface to the detector can explain the data reported here. Similarly, our results could not be caused by some event which occurred at a fixed time each day. The rotation of the earth provides an unquestionable form of signal averaging for this type of experiment.

In summary, we have found no systematic problems with the data.

VIII. CONCLUSIONS

We have observed apparent anisotropies and inhomogeneities in the flux of multimuon events which are not likely to have been caused by statistical fluctuations of an isotropic and random background. In the time-integrated data, we observe small enhancements in a pattern which appears related to the orientation of the local Milky Way galaxy. In the time-dependent data analysis, we observe episodic bursts of multimuon events coming mostly from a specific direction in the vicinity of Cygnus X-3. However, the single-muon data do not show such an effect. After considerable analysis effort, we have not been able to find systematic errors which would explain these effects. However, because of the lack of *a priori* hypotheses, it is difficult to assign a precise statistical significance to the reported results. In any case, we believe that it is useful to

report these data, so that subsequent experiments will have some predetermined hypotheses whose validity can be tested.

If the anomalies reported here are indeed correct, these data will have considerable consequence for our understanding of the local galactic environment. Because the primaries detected in these anomalies show angular dispersion and because they create muons, it is likely that they are charged. They must then either have a higher energy than expected from conventional flux-energy relations, have been emitted by a nearby galactic source or have experienced a reduced galactic magnetic field. The regions of space with a reduced magnetic field could well be localized in space, time or both.

The new generation of proton-decay detectors[18] should provide an order of magnitude increase in statistics which will quickly either confirm or deny effects of the type we are reporting. If such effects are confirmed, these new detectors will then have considerable value as astrophysical probes, in addition to their intended use in the search for proton decay.

* Present address: Stanford Linear Accelerator Center, P. O. Box 4349, Stanford, CA 94305.

† Permanent address: Tata Institute of Fundamental Research, Bombay 40 00 05, India.

1 G. R. Smith, M. Ogmen, E. Buller, and S. Standil, Phys. Rev. D **28**, 1601 (1983). This paper also contains references to earlier searches for time-dependent effects.

2 M. Samorski and W. Stamm, Astrophys. J. Lett. **268**, L17 (1983).

3 J. Lloyd-Evans *et al.*, Nature **305**, 784 (1983), and other papers listed in this reference.

4 J. Dickey, Astrophys. J. **273**, L71 (1983).

5 R. Protheroe *et al.*, Astrophys. J. Lett. **280**, L47 (1984).

6 G. Smith *et al.*, Phys. Rev. Lett. **50**, 2110 (1983).

7 D. Fegan *et al.*, Phys. Rev. Lett. **51**, 2341 (1983).

8 B. J. Geldzahler *et al.*, Astrophys. J. Lett. **273**, L65 (1983).

9 J. Bartelt, Ph.D. thesis, Univ. of Minnesota, 1984; J. Bartelt *et al.*, Phys. Rev. Lett. **50**, 651 and 655 (1983).

10 T. Gaisser and G. Yodh, Ann. Rev. Nucl. Part. Sci. **30**, 475 (1980).

11 T. Stanev, private communication.

12 G. H. Lowe *et al.*, Phys. Rev. D **12**, 651 (1975).

13 M. R. Krishnaswamy *et al.*, in *Proceedings of the Fifteenth International Conference on Cosmic Rays, Plovdiv, Bulgaria, 1977*, edited by B. Betev (Bulgarian Academy of Sciences, Sofia, 1977), Vol. 6, p. 85.

14 D. J. Cutler *et al.*, Astrophys. J. **248**, 1166 (1981).

15 M. G. K. Menon and P. V. Ramana Murthy, Prog. Elem. Part. Cosmic Ray Phys. **IX**, 161 (1967).

16 T. Kobayakawa, in *Proceedings of the 13th International Cosmic Ray Conference, Denver, 1973*, edited by R. L. Chasson (University of Colorado, Boulder, 1973), p. 3156.

17 M. van der Klis and J. M. Bonnet-Bidaud, Astron. and Astrophys. **95**, L5 (1981).

18 A brief description of the new generation of proton-decay detectors is given by L Sulak, in *Proceedings of the 21st International Conference on High Energy Physics, Paris, 1982*, edited by P. Petiau and M. Porneuf [J. Phys. (Paris) Colloq. **43**, C3-205 (1982)].